Electronic Supplementary Material (ESI) for New Journal of Chemistry.

Pnictogen Bonding with Alkoxide Cages: Which Pnictogen is Best?

*Henry J. Trubenstein,† Shiva Moaven,† Maythe Vega, Daniel K. Unruh and Anthony F. Cozzolino**

Supplementary Information

† denotes equal contribution

Department of Chemistry and Biochemistry, Texas Tech University, Box 1061, Lubbock, Texas 79409-1061, United States

Table of Contents

S1 Experimental Details

S1.1 General Methods

The starting materials, arsenic trichloride (Strem, 99%), sodium ethoxide (Alfa Aesar, 96%), 1,1,1–trimethylolpropane(Merck, 98%), and 1,1,1–trimethylolethane (Alfa Aesar, 98%), bismuth trichloride (Strem, 99.9%), lithium dimethylamide (Sterm, 98%) were used as purchased. Bismuth dimethyl amide was prepared based on reported previously.[1] Anhydrous tetrahydrofuran was obtained by passing HPLC grade tetrahydrofuran over a bed of activated molecular sieves in a commercial (LC Technologies Solutions Inc.) solvent purification system (SPS). Deuterated solvents, purchased from Cambridge Isotopes Laboratory, were degassed using three freeze-pump-thaw cycles before being transferred onto freshly activated molecular sieves. Air sensitive manipulations were performed in an N_2 purged inert atmosphere box (LC Technology Solutions Inc.). All NMR spectra were collected on a JEOL ECS 400 MHz NMR spectrometer. All IR spectra were obtained using a Nicolet iS 5 FT-IR spectrometer equipped with a Specac Di Quest ATR accessory, and CHN analysis were obtained either on-site with a Perkin Elmer 2400 Series II CHNS/O analyzer.

S1.2 Synthesis

S1.2.1 Preparation of arsenic triethoxide

This preparation was adapted from the previously reported synthesis of antimony tris(t-butoxide) in our previous work.[2] All manipulations were performed under a nitrogen gas atmosphere. Sodium ethoxide (12.2 g; 179 mmol) was added to a 150 mL round bottom flask. The flask was cooled down to −78 °C in a cold well. THF (50 mL) was added to the solid. Arsenic trichloride (5.03 mL; 60.1 mmol) was dissolved in THF (50 mL) and cooled down to −35 °C in a freezer. The arsenic

solution was then added slowly to the solution within the round bottom flask. The resulting solution was stirred and maintained room temperature for 24 hours. All volatiles were then removed under vacuum. Hexanes (100 mL) were added to the product vessel and the solution was then filtered. All volatiles were removed under vacuum once more. Yield: 6.58 g (52.2%, 31.3 mmol). ^{1}H NMR (Benzene-d_6, δ ppm) 3.79 (q, 5H), 1.12 (t, 10H). ^{13}C NMR (Benzene-d_6, δ ppm) 58.48, 18.38. Di-ATR-FTIR (cm^{-1}): 2971 (s, ν_{C-H}) 1023 (vs, ν_{C-O}) 604 (m, ν_{As-O}).

S1.2.2 Synthesis of $As(OCH_2)_3CCH_3$ (**2**-As)

All manipulations were performed under a nitrogen gas atmosphere. Arsenic triethoxide (0.230 g; 1.09 mmol) was dissolved in THF (5 mL) within a small vial. After the solid dissolved, 1,1,1-trimethylolethane (0.140 g; 1.17 mmol) was added to the vial and the solution was stirred for 1 hour at room temperature. The volatile components were then removed under vacuum. The crude product was dissolved in hexanes (5 mL) then cooled down to −35 °C in a freezer for 3 hours to yield colorless crystals. The solution was decanted and then the volatiles were removed by vacuum. Yield: 0.124 g (59.0%, 0.646 mmol). mp 38-41 °C. ^{1}H NMR (Chloroform-*d,* δ ppm) 4.04 (s, 6H), 0.65 (s, 3H). ^{13}C NMR (Chloroform-*d,* δ ppm) 73.95, 33.46, 17.45. Di-ATR-FTIR (cm^{-1}): 2963 (m, ν_{C-H}), 2931 (m, ν_{C-H}), 2865 (s, ν_{C-H}), 1010 (s, ν_{C-O}) 583 (vs, ν_{As-O}). Calc. (% C, % H): 31.27, 4.72. Exp. (% C, % H): 31.43, 4.59.

S1.2.3 Synthesis of $As(OCH_2)_3CCH_2CH_3$ (**3**-As)

All manipulations were performed under a nitrogen gas atmosphere. Arsenic triethoxide (0.215 g; 1.02 mmol) was dissolved in THF (5 mL) within a small vial. After the solid dissolved, 1,1,1-trimethylolpropane (0.136 g; 1.01 mmol) was added to the vial and the solution was stirred for one

hour at room temperature. The volatile components were removed under vacuum. The crude product was dissolved in hexanes (5 mL) then cooled down to −35 °C in a freezer for 3 hours to yield colorless crystals. The solution was decanted and then the volatiles were removed by vacuum. Yield: 0.123 g (58.9%, 0.597 mmol). mp 47-50 °C. ^{1}H NMR (Chloroform-*d*, δ ppm) 4.07 (s, 6H), 1.09 (q, J = 7.7 Hz, 2H), 0.78 (t, J = 7.9 Hz, 3H). ^{13}C NMR (Chloroform-*d*, δ ppm) 72.51, 35.77, 25.24, 7.31. Di-ATR-FTIR (cm^{-1}): 2974 (m, ν_{C-H}), 2925 (m, ν_{C-H}), 2859 (s, ν_{C-H}), 1030 (s, ν_{C-O}) 581 (s, ν_{As-O}). Calc. (% C, % H): 34.97, 5.38. Exp. (% C, % H): 34.84, 5.54.

S1.2.4 Synthesis of $Bi(OCH_2)_3CCH_3$ (**2**-Bi)

The preparation of **2**-Bi was attempted in both solution and the solid-state(neat/grinding). The ones that yielded the cleanest materials are highlighted in Table S1 and are reported in more detail below.

Table S1. Summary of different attempts for preparation of **2**-Bi.

	THF	Pyridine	DMF	DMSO	Neat (Grinding)
$Bi(NMe_2)_3$	solid	solid	gel	gel	solid
$Bi(O^tBu)_3$	solid	solid	gel	gel	—

Method A: In 5 mL of dry THF 0.120 g (0.999 mmol) of 1,1,1-trimethylolethane was dissolved and while it was stirring 2 mL THF solution containing 0.341 g (0.999 mmol) of bismuth(III) dimethyl amide was added to it. Upon the addition of the bismuth reagent a white precipitate rapidly formed. The solvent was evaporated under vacuum and 0.292 g of white solid was recovered. mp: decomposed at 255 °C. Di-ATR-FTIR (cm^{-1}): 2943 (s, ν_{C-H}), 2825 (s, ν_{C-H}), 1052 (vs, ν_{C-O}), 502 (s, ν_{Bi-O}), 489 (s, ν_{Bi-O}), 473 (s, ν_{Bi-O}).

Method B: In 5 mL of dry THF 0.120 g (0.999 mmol) of 1,1,1-trimethylolethane was dissolved and while it was stirring 2 mL THF solution containing 0.428 (0.999 mmol) g of bismuth(III) *tert*-

butoxide was added to it. Upon the addition of the bismuth reagent a white precipitate rapidly formed. The solid was filtered under vacuum and 0.368 g of beige color solid was recovered. mp: decomposed at 255 °C. Di-ATR-FTIR (cm^{-1}): 2944 (s, ν_{C-H}), 2828 (s, ν_{C-H}), 1057 (vs, ν_{C-O}), 517 (s, ν_{Bi-O}), 491 (s, ν_{Bi-O}).

Method C: Inside glovebox under inert N_2 atmosphere, 0.120 g (0.999 mmol) of 1,1,1-trimethylolethane and 0.341 (0.999 mmol) g of bismuth (III) dimethyl amide were added to an agar mortar. Two solids were gently mixed via the pestle into each other until the mixture looked homogeneous (yellow), and then more pressure was applied until release of the dimethyl amine gas was observed, the mixture was grinded until the mixture became milky-white. To confirm completion of the reaction IR was used to probe disappearance of the O–H stretching band of the alcohol. The solid was not soluble in polar solvents. Di-ATR-FTIR (cm^{-1}): 2959 (s, ν_{C-H}), 2819 (s, ν_{C-H}), 1062 (vs, ν_{C-O}), 518 (s, ν_{Bi-O}), 493 (s, ν_{Bi-O}), 480 (s, ν_{Bi-O}).

S1.2.5 Synthesis of $Bi(OCH_2)_3CCH_2CH_3$ (**3**-Bi)

The preparation of **3**-Bi was attempted in both solution and the solid-state(neat/grinding). The conditions that yielded the cleanest materials are highlighted in Table S2 and are reported in more detail below.

Table S2. Summary of different attempts for preparation of **3**-Bi.

	THF	Pyridine	DMF	DMSO	Neat (Grinding)
$Bi(NMe_2)_3$	solid	solid	gel	gel	solid
$Bi(O^tBu)_3$	solid	solid	gel	gel	—

Method A: In 5 mL of dry THF 0.134 g (0.999 mmol) of 1,1,1-trimethylolpropane was dissolved and while it was stirring 2 mL THF solution containing 0.341 g (0.999 mmol) of bismuth(III) dimethyl amide was added to it. Upon the addition of the bismuth reagent a white precipitate

rapidly formed. The solvent was evaporated under vacuum and 0.292 g of white solid was recovered. mp: decomposed at 255 °C. Di-ATR-FTIR (cm^{-1}): 2959 (s, $\nu_{C–H}$), 2820 (s, $\nu_{C–H}$), 1063 (vs, $\nu_{C–O}$), 517 (s, $\nu_{Bi–O}$), 492 (s, $\nu_{Bi–O}$), 470 (s, $\nu_{Bi–O}$).

Method B: In 5 mL of dry THF 0.134 g (0.999 mmol) of 1,1,1-trimethylolethane was dissolved and while it was stirring 2 mL THF solution containing 0.428 g (0.999 mmol) of bismuth(III) *tert*-butoxide was added to it. Upon the addition of the bismuth reagent a white precipitate rapidly formed. The solid was filtered under vacuum and 0.423 g of beige color solid was recovered. mp: decomposed at 255 °C. Di-ATR-FTIR (cm^{-1}): 2961 (s, $\nu_{C–H}$), 2806 (s, $\nu_{C–H}$), 1059 (vs, $\nu_{C–O}$), 480 (b, $\nu_{Bi–O}$).

Method C: Inside glovebox under inert N_2 atmosphere, 0.134 g (0.999 mmol) of 1,1,1-trimethylolethane and 0.341 g (0.999 mmol) of bismuth (III) dimethyl amide were added to an agar mortar. Two solids were gently mixed via the pestle into each other until the mixture looked homogeneous (yellow), and then more pressure was applied until release of the dimethyl amine gas was observed the mixture was grinded until the mixture became milky-white. To confirm completion of the reaction IR was used to probe disappearance of the O–H stretching band of the alcohol. The solid was not soluble in polar solvents. Di-ATR-FTIR (cm^{-1}): 2959 (s, $\nu_{C–H}$), 2819 (s, $\nu_{C–H}$), 1062 (vs, $\nu_{C–O}$), 518 (s, $\nu_{Bi–O}$), 493 (s, $\nu_{Bi–O}$), 480 (s, $\nu_{Bi–O}$).

S1.3 Crystallography

Single crystals of **2**-As and **3**-As were prepared by introducing a saturated anhydrous hexanes solution of **2**-As or **3**-As into a –35 °C freezer under nitrogen. Diffraction quality crystals grew overnight.

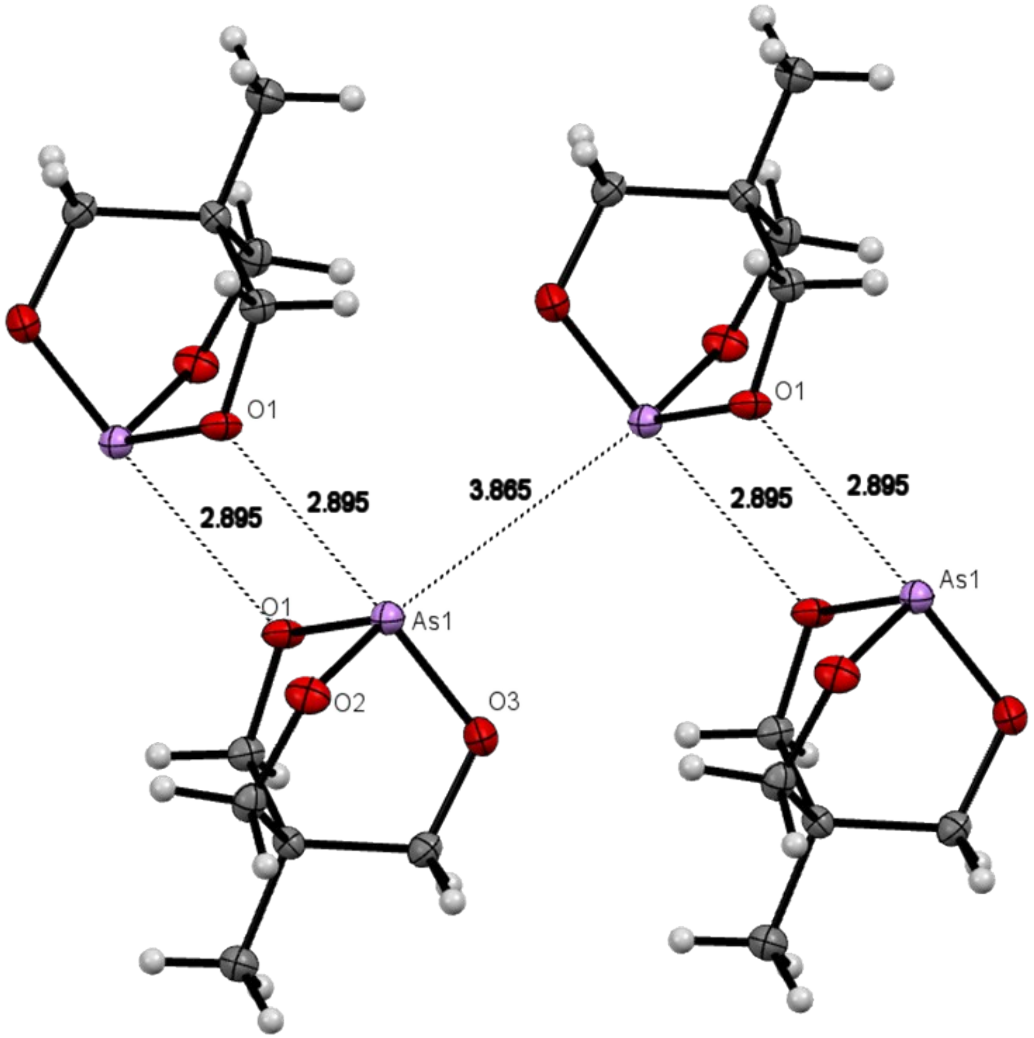

Figure S1. The thermal ellipsoids of **2**-As are represented at 50% probability. Carbon, hydrogen, oxygen, and arsenic atoms are represented in gray, white, red, and purple, respectively.

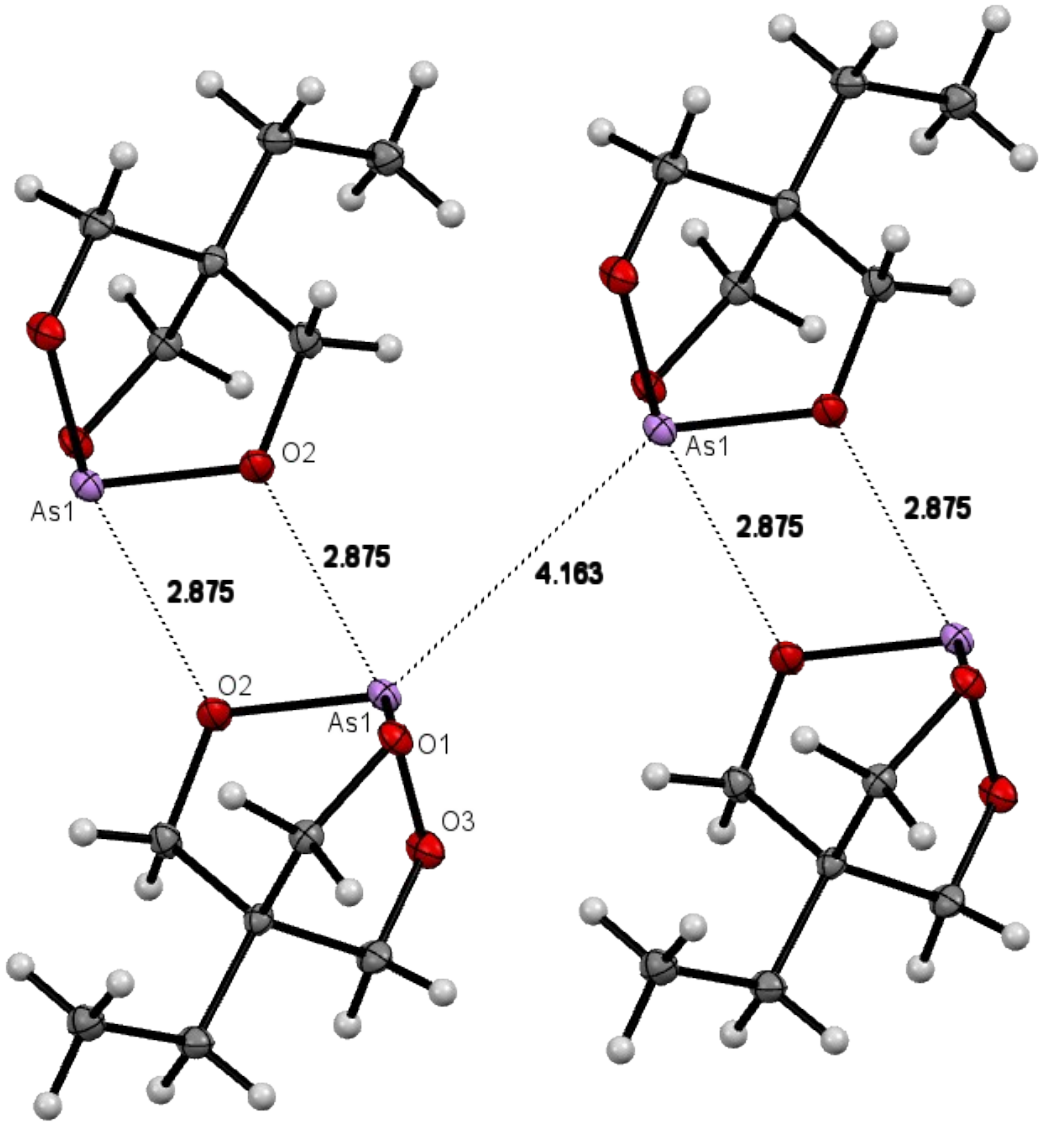

Figure S2. The thermal ellipsoids of **3**-As are represented at 50% probability. Carbon, hydrogen, oxygen, and arsenic atoms are represented in gray, white, red, and purple, respectively.

Table S3. Crystal data and structure refinement for **2**-As and **3**-As.

Structure	**2**-As	**3**-As
Crystal Color	colorless	colorless
Crystal Habit	blade	block
Empirical formula	$C_5H_9AsO_3$	$C_6H_{11}AsO_3$
Formula weight (g/mol)	192.04	206.07
Temperature	100(2) K	100(2) K
Wavelength	0.71073 Å	0.71073 Å
Crystal system	Monoclinic	Monoclinic
Space group	$P2_1/n$	$P2_1/n$
Unit cell dimensions	a = 5.992(2) Å b = 10.546(3) Å c = 10.779(3) Å α = 90° β = 100.379(4)° γ = 90°	a = 6.018(2) Å b = 11.627(5) Å c = 10.644(4) Å α = 90° β = 92.280(6)° γ = 90°
Volume	670.0(3) $Å^3$	744.1(5) $Å^3$
Z	4	4
Calculated density	1.904 g/cm^3	1.839 g/cm^3
Absorption coefficient	5.003 mm^{-1}	4.512 mm^{-1}
F(000)	384	416
Crystal size	0.220 × 0.050 × 0.010 mm	0.475 × 0.425 × 0.400 mm
Theta range for data collection	2.724 to 26.538°	2.595 to 27.117°
Limiting indices	$-7 \leq h \leq 7$ $-12 \leq k \leq 13$ $-13 \leq l \leq 13$	$-7 \leq h \leq 7$ $-14 \leq k \leq 14$ $-13 \leq l \leq 13$
Reflections collected / unique	5947/1387 [R(int) = 0.0499]	8373/1643 [R(int) = 0.0189]
Completeness to theta = 25.242°	100.0%	100.0%
Refinement method	Full-matrix least-squares on F^2	Full-matrix least-squares on F^2
Data / restraints / parameters	1387/0/83	1643/0/92
Goodness-of-fit on F^2	1.037	1.076
Final R indices [I>2sigma(I)]	R1 = 0.0293, wR2 = 0.0546	R1 = 0.0158, wR2 = 0.0380
R indices (all data)	R1 = 0.0455, wR2 = 0.0588	R1 = 0.0177, wR2 = 0.0385
Largest diff. peak and hole	0.411 and −0.507 $e \cdot Å^{-3}$	0.409 and −0.237 $e \cdot Å^{-3}$

Table S4. Atomic coordinates ($\times 10^4$) and equivalent isotropic displacement parameters ($Å^2 \times 10^3$) for **2**-As. $U_{(eq)}$ is defined as one third of the trace of the orthogonalized U_{ij} tensor.

	x	y	z	$U_{(eq)}$
As(1)	2691(1)	4107(1)	695(1)	17(1)
O(1)	983(4)	5224(2)	1331(2)	18(1)
O(2)	1156(4)	2728(2)	954(2)	21(1)
O(3)	4825(4)	3979(3)	2068(2)	25(1)
C(1)	612(6)	4979(3)	2605(3)	16(1)
C(2)	375(5)	2664(3)	2149(3)	17(1)
C(3)	4057(5)	3625(3)	3208(3)	18(1)
C(4)	1462(5)	3674(3)	3088(3)	13(1)
C(5)	853(6)	3418(4)	4367(3)	21(1)

Table S5. Bond lengths [Å] and angles [°] for **2**-As.

As(1)-O(2)	1.770(2)
As(1)-O(1)	1.777(2)
As(1)-O(3)	1.778(2)
O(1)-C(1)	1.453(4)
O(2)-C(2)	1.449(4)
O(3)-C(3)	1.437(4)
C(1)-C(4)	1.526(5)
C(1)-H(1A)	0.9900
C(1)-H(1B)	0.9900
C(2)-C(4)	1.532(4)
C(2)-H(2A)	0.9900
C(2)-H(2B)	0.9900
C(3)-C(4)	1.538(4)
C(3)-H(3A)	0.9900
C(3)-H(3B)	0.9900
C(4)-C(5)	1.512(5)
C(5)-H(5A)	0.9800
C(5)-H(5B)	0.9800
C(5)-H(5C)	0.9800
O(2)-As(1)-O(1)	97.57(11)
O(2)-As(1)-O(3)	97.03(11)
O(1)-As(1)-O(3)	96.13(11)
C(1)-O(1)-As(1)	116.33(19)
C(2)-O(2)-As(1)	116.0(2)
C(3)-O(3)-As(1)	116.04(19)
O(1)-C(1)-C(4)	112.6(3)
O(1)-C(1)-H(1A)	109.1
C(4)-C(1)-H(1A)	109.1
O(1)-C(1)-H(1B)	109.1
C(4)-C(1)-H(1B)	109.1
H(1A)-C(1)-H(1B)	107.8
O(2)-C(2)-C(4)	112.8(3)

O(2)-C(2)-H(2A)	109.0
C(4)-C(2)-H(2A)	109.0
O(2)-C(2)-H(2B)	109.0
C(4)-C(2)-H(2B)	109.0
H(2A)-C(2)-H(2B)	107.8
O(3)-C(3)-C(4)	113.2(3)
O(3)-C(3)-H(3A)	108.9
C(4)-C(3)-H(3A)	108.9
O(3)-C(3)-H(3B)	108.9
C(4)-C(3)-H(3B)	108.9
H(3A)-C(3)-H(3B)	107.8
C(5)-C(4)-C(1)	110.6(3)
C(5)-C(4)-C(2)	109.6(3)
C(1)-C(4)-C(2)	109.0(3)
C(5)-C(4)-C(3)	108.9(3)
C(1)-C(4)-C(3)	109.2(3)
C(2)-C(4)-C(3)	109.6(3)
C(4)-C(5)-H(5A)	109.5
C(4)-C(5)-H(5B)	109.5
H(5A)-C(5)-H(5B)	109.5
C(4)-C(5)-H(5C)	109.5
H(5A)-C(5)-H(5C)	109.5
H(5B)-C(5)-H(5C)	109.5

Table S6 Atomic coordinates ($\times 10^4$) and equivalent isotropic displacement parameters ($Å^2 \times 10^3$) for **3**-As. $U_{(eq)}$ is defined as one third of the trace of the orthogonalized U_{ij} tensor.

	x	y	z	$U_{(eq)}$
As(1)	7259(1)	4404(1)	3937(1)	13(1)
O(1)	7660(2)	3187(1)	4936(1)	14(1)
O(2)	4286(2)	4409(1)	3895(1)	15(1)
O(3)	7527(2)	3645(1)	2490(1)	17(1)
C(1)	6003(3)	2287(1)	4768(1)	12(1)
C(2)	3230(3)	3370(1)	3416(2)	14(1)
C(3)	6555(3)	2501(1)	2460(2)	15(1)
C(4)	4811(2)	2336(1)	3465(1)	11(1)
C(5)	3547(3)	1211(1)	3182(2)	15(1)
C(6)	1898(3)	844(1)	4171(2)	17(1)

Table S7 Bond lengths [Å] and angles [°] for **3**-As.

As(1)-O(1)	1.7809(12)
As(1)-O(2)	1.7876(13)
As(1)-O(3)	1.7882(13)
O(1)-C(1)	1.4519(18)
O(2)-C(2)	1.4481(19)
O(3)-C(3)	1.453(2)
C(1)-C(4)	1.537(2)

C(1)-H(1A)	0.9900
C(1)-H(1B)	0.9900
C(2)-C(4)	1.533(2)
C(2)-H(2A)	0.9900
C(2)-H(2B)	0.9900
C(3)-C(4)	1.540(2)
C(3)-H(3A)	0.9900
C(3)-H(3B)	0.9900
C(4)-C(5)	1.537(2)
C(5)-C(6)	1.535(2)
C(5)-H(5A)	0.9900
C(5)-H(5B)	0.9900
C(6)-H(6A)	0.9800
C(6)-H(6B)	0.9800
C(6)-H(6C)	0.9800

O(1)-As(1)-O(2)	97.41(5)
O(1)-As(1)-O(3)	96.17(6)
O(2)-As(1)-O(3)	96.01(5)
C(1)-O(1)-As(1)	115.03(9)
C(2)-O(2)-As(1)	115.52(9)
C(3)-O(3)-As(1)	114.88(9)
O(1)-C(1)-C(4)	112.21(12)
O(1)-C(1)-H(1A)	109.2
C(4)-C(1)-H(1A)	109.2
O(1)-C(1)-H(1B)	109.2
C(4)-C(1)-H(1B)	109.2
H(1A)-C(1)-H(1B)	107.9
O(2)-C(2)-C(4)	112.28(12)
O(2)-C(2)-H(2A)	109.1
C(4)-C(2)-H(2A)	109.1
O(2)-C(2)-H(2B)	109.1
C(4)-C(2)-H(2B)	109.1
H(2A)-C(2)-H(2B)	107.9
O(3)-C(3)-C(4)	112.58(13)
O(3)-C(3)-H(3A)	109.1
C(4)-C(3)-H(3A)	109.1
O(3)-C(3)-H(3B)	109.1
C(4)-C(3)-H(3B)	109.1
H(3A)-C(3)-H(3B)	107.8
C(2)-C(4)-C(1)	109.05(12)
C(2)-C(4)-C(5)	111.08(13)
C(1)-C(4)-C(5)	110.76(12)
C(2)-C(4)-C(3)	108.51(13)
C(1)-C(4)-C(3)	108.98(12)
C(5)-C(4)-C(3)	108.40(12)
C(6)-C(5)-C(4)	115.51(13)
C(6)-C(5)-H(5A)	108.4
C(4)-C(5)-H(5A)	108.4
C(6)-C(5)-H(5B)	108.4
C(4)-C(5)-H(5B)	108.4
H(5A)-C(5)-H(5B)	107.5
C(5)-C(6)-H(6A)	109.5
C(5)-C(6)-H(6B)	109.5

H(6A)-C(6)-H(6B)	109.5
C(5)-C(6)-H(6C)	109.5
H(6A)-C(6)-H(6C)	109.5
H(6B)-C(6)-H(6C)	109.5

S1.4 Computational Method

Calculations were performed using the ORCA 4.0 quantum chemistry program package from the development team at the Max Planck Institute for Bioinorganic Chemistry.[3] The starting geometry for optimization of **1**-Pn was adapted from the corresponding crystal structures of **1**-Pn; the antimony structure was used for **1**-Bi. All calculations were carried out using the Zero-Order Regular Approximation (ZORA).[4,5] For geometry optimizations, frequencies, and thermochemistry the B97-D3[6] functional and def2-TZVPP[7,8] with SARC/J basis sets[9] were used for hydrogen atoms and all other atoms respectively. Spin-restricted Kohn– Sham determinants[10] were chosen to describe the closed shell wavefunctions, employing the RI approximation[11] and the tight SCF convergence criteria provided by ORCA. The basis set superposition error (BSSE) was corrected using the Boys and Bernardi procedures.[12] Molecular electrostatic potential (ESP) mapping was performed on the 0.001 isosurface of the electron density using the Multiwfn program.[13,14] All visualizations of ESP maps were performed with the Gabedit graphical interface software.[15] The cartesian coordinates of the geometry optimized molecules and supramolecules are provided as .xyz files in a .zip file.

S2 Spectroscopic Data

S2.1 ^{1}H NMR

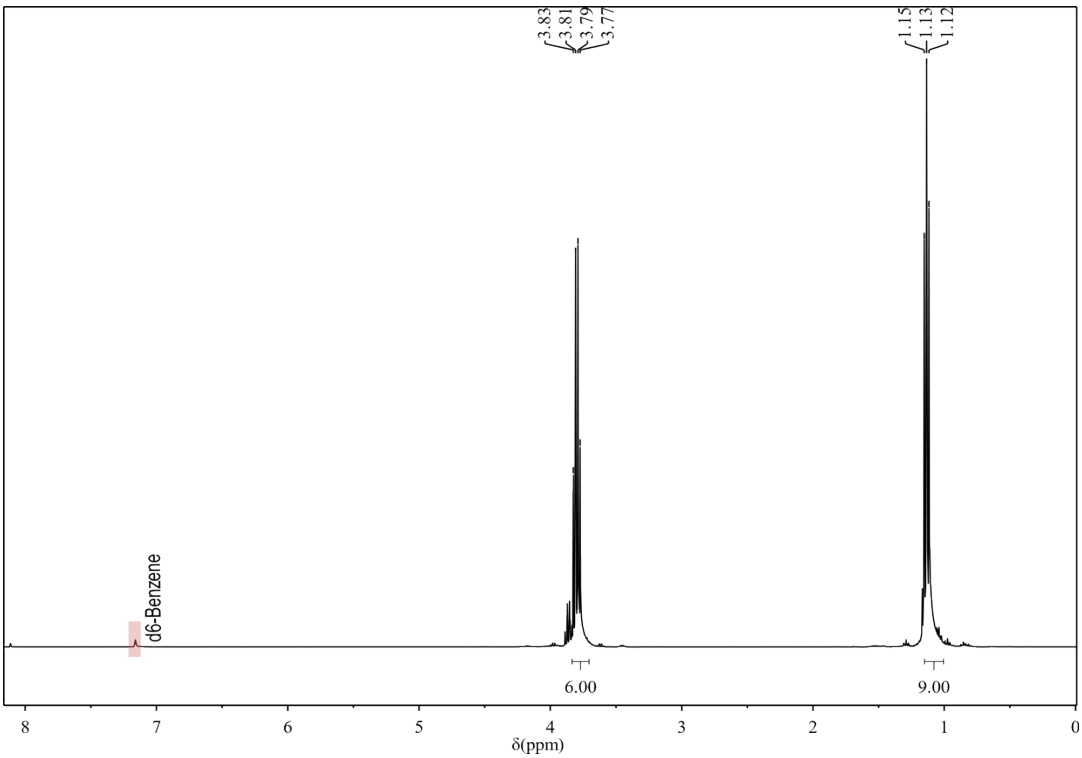

Figure S3. ^{1}H NMR of arsenic triethoxide.

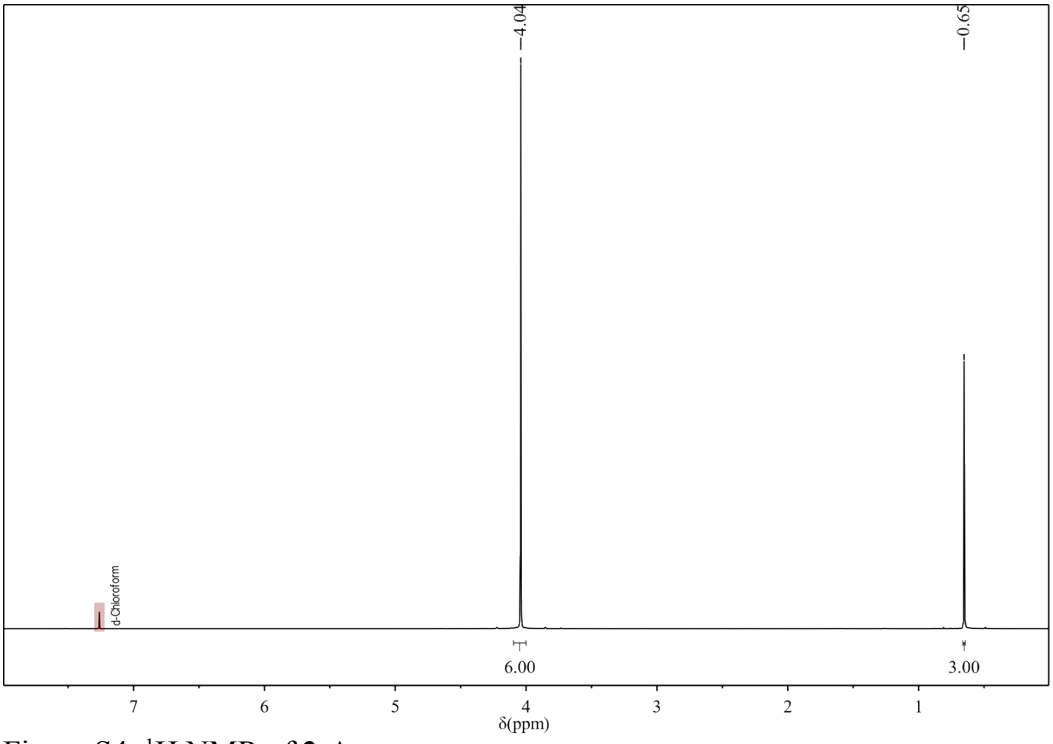

Figure S4. ^{1}H NMR of **2**-As.

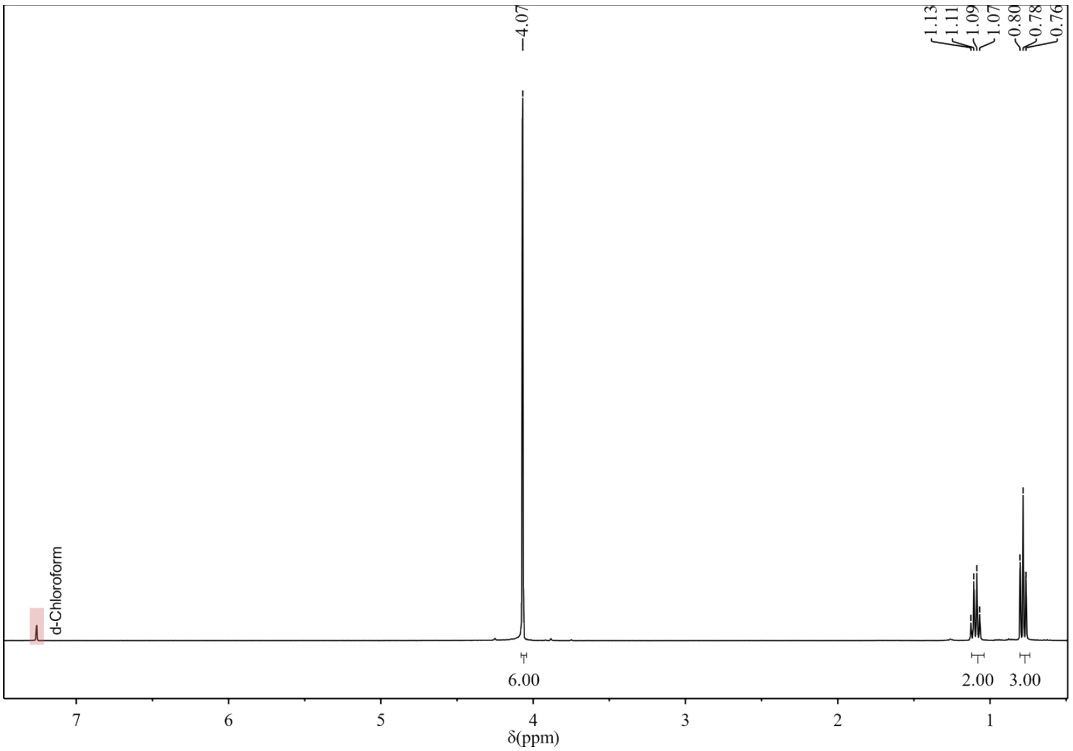

Figure S5. ^{1}H NMR of **3**-As.

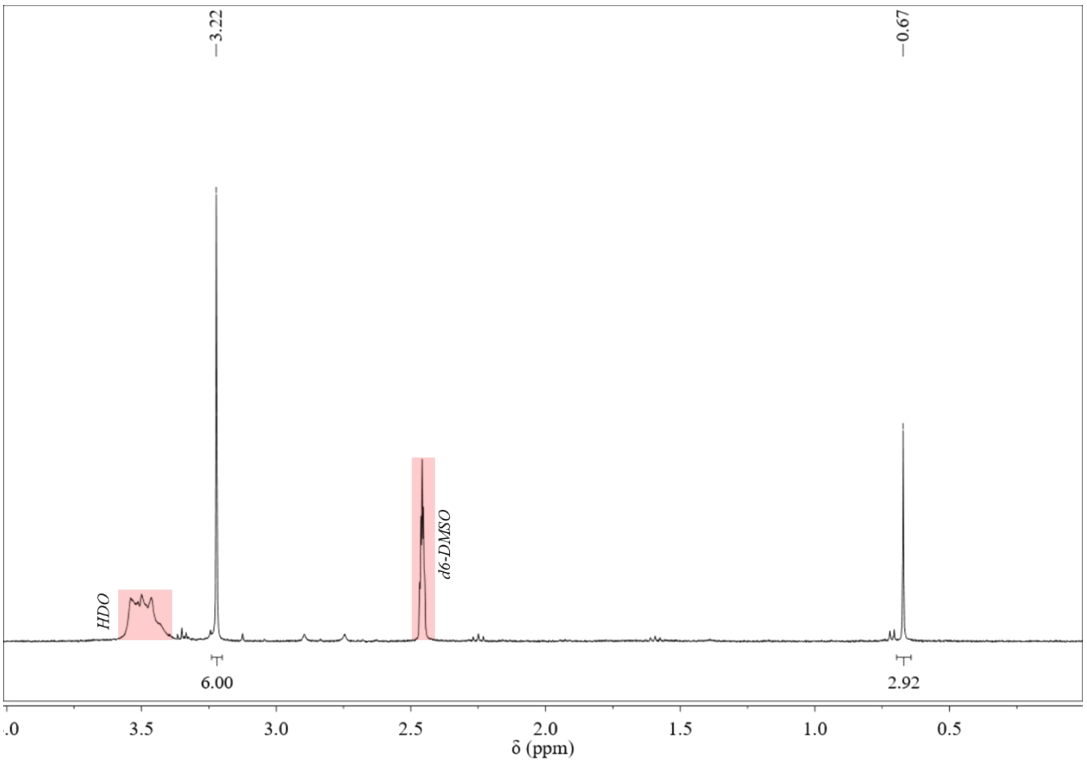

Figure S6. ^{1}H NMR of hydrolysis of **2**-Bi (prepared with Method A).

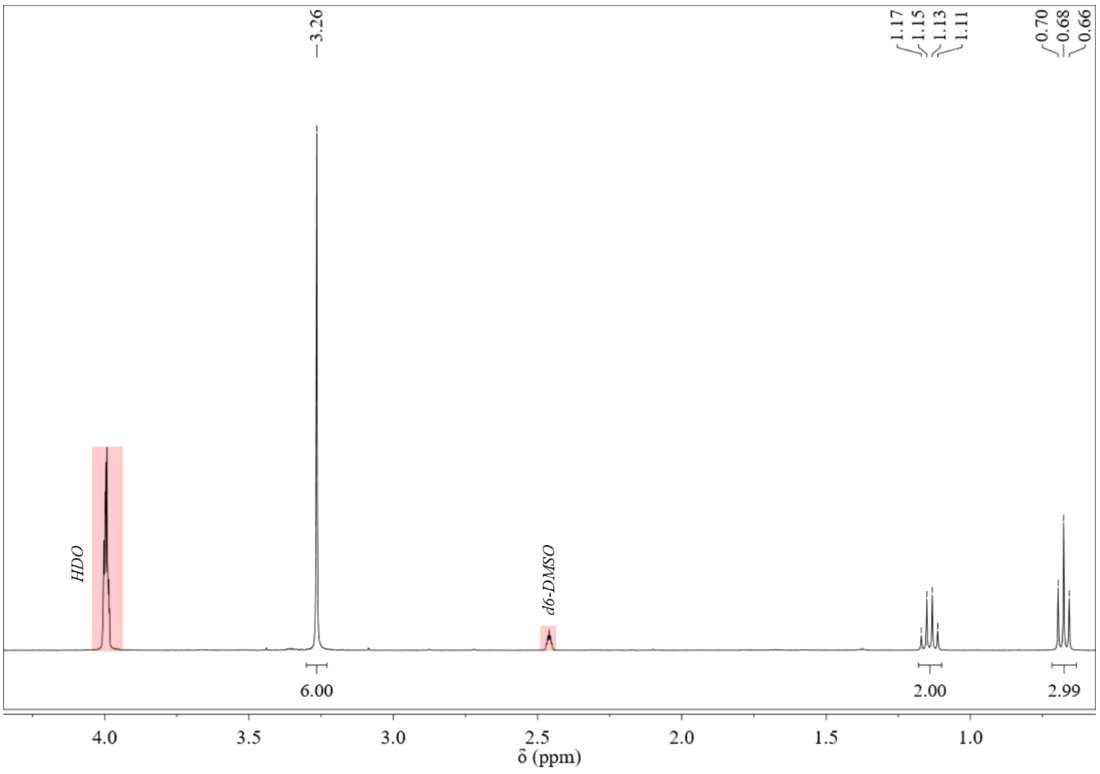

Figure S7. ^{1}H NMR of hydrolysis of **3**-Bi (prepared with Method A).

S2.2 $^{13}C\{^{1}H\}$ NMR

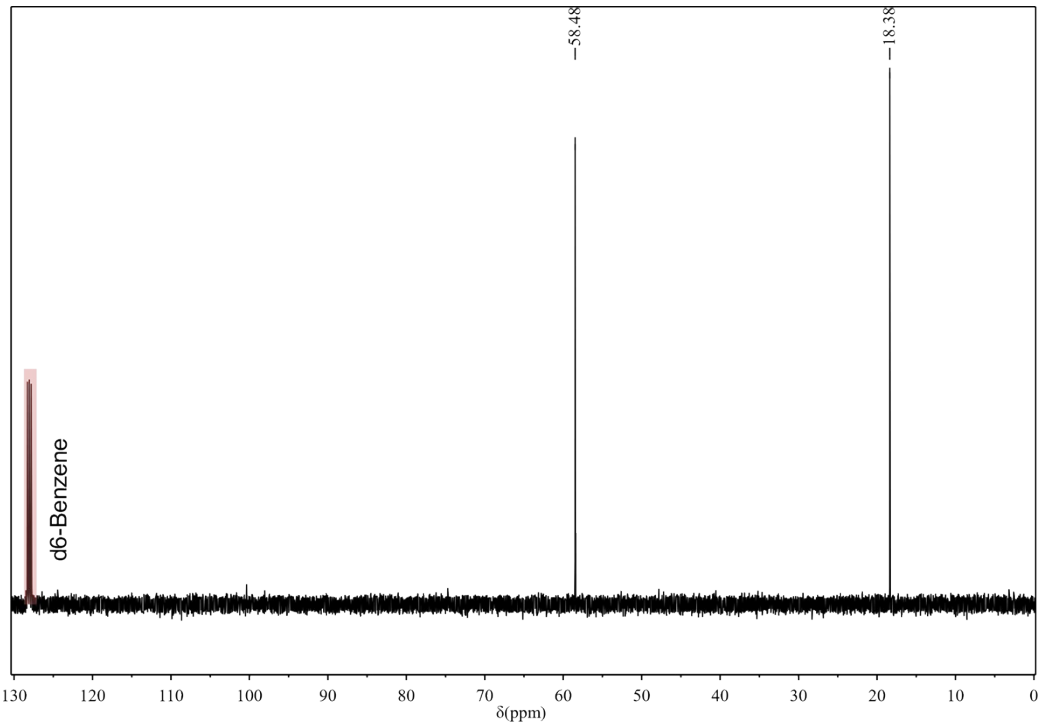

Figure S8. $^{13}C\{^{1}H\}$ NMR of arsenic triethoxide.

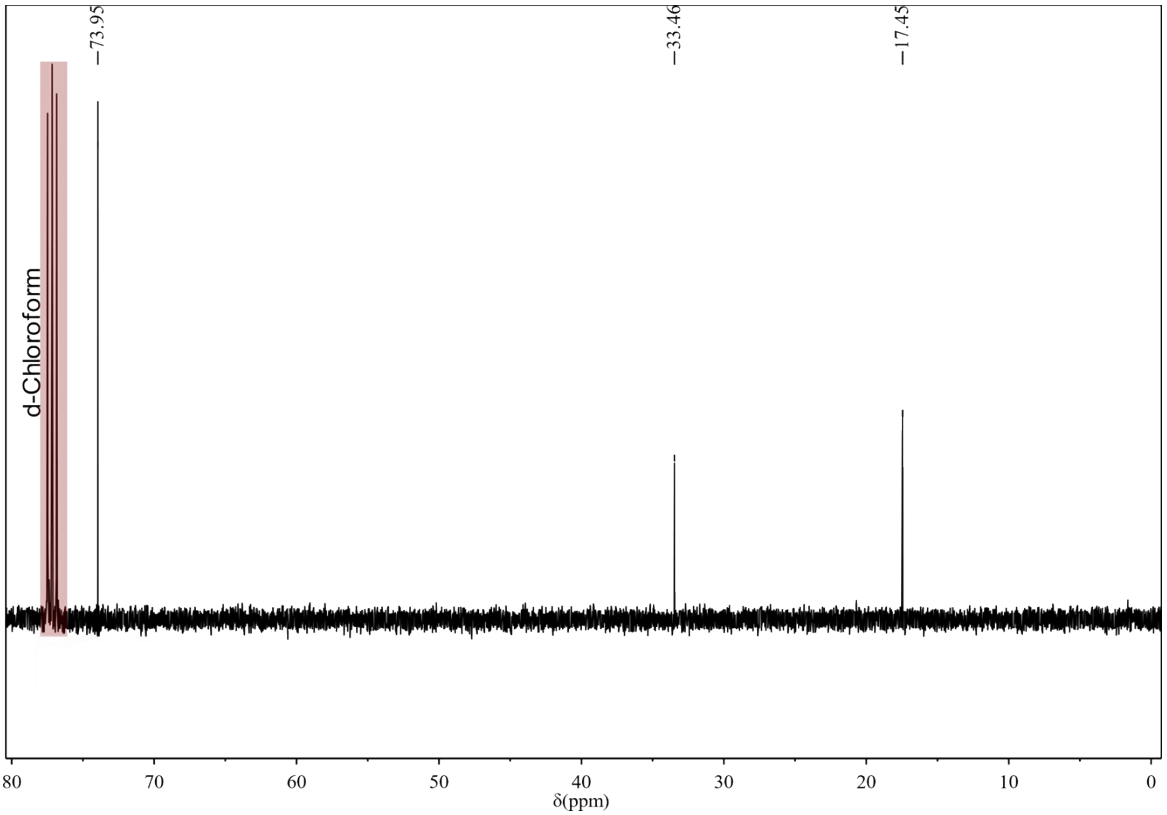

Figure S9. $^{13}C\{^{1}H\}$ NMR of **2**-As.

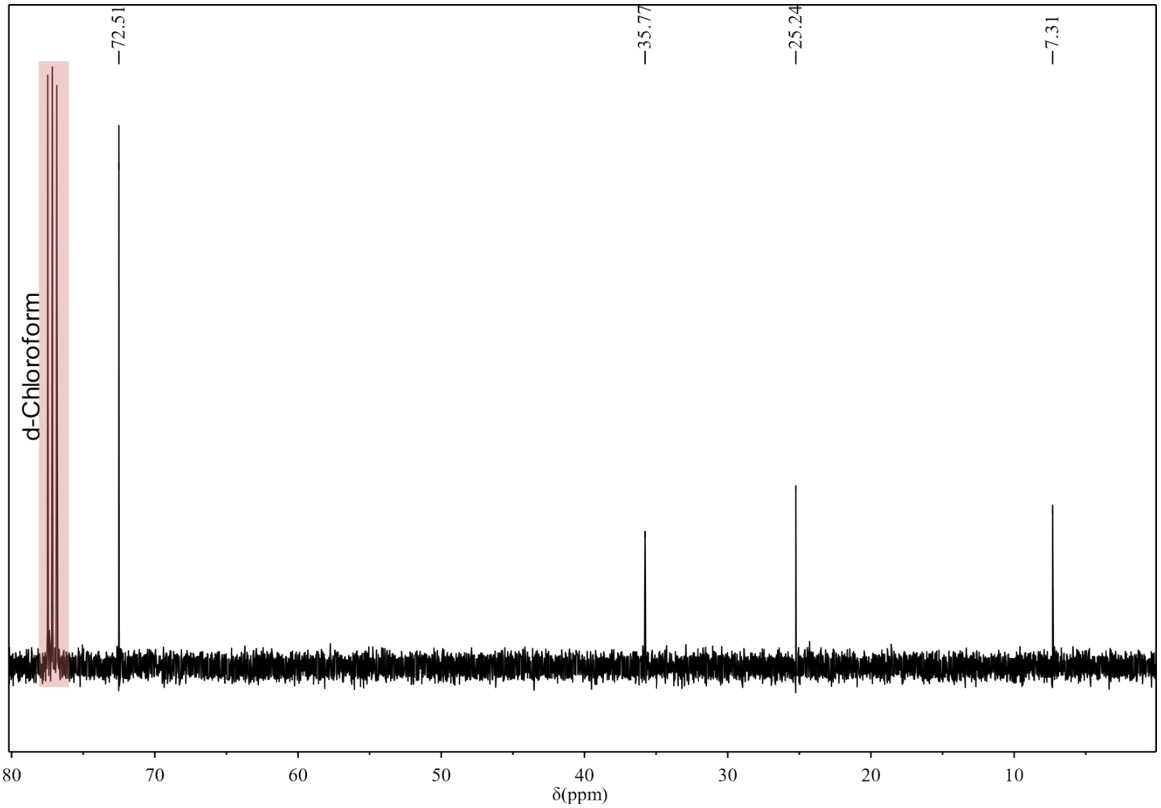

Figure S10. $^{13}C\{^{1}H\}$ NMR of **3**-As.

S2.3 Di-ATR-FTIR

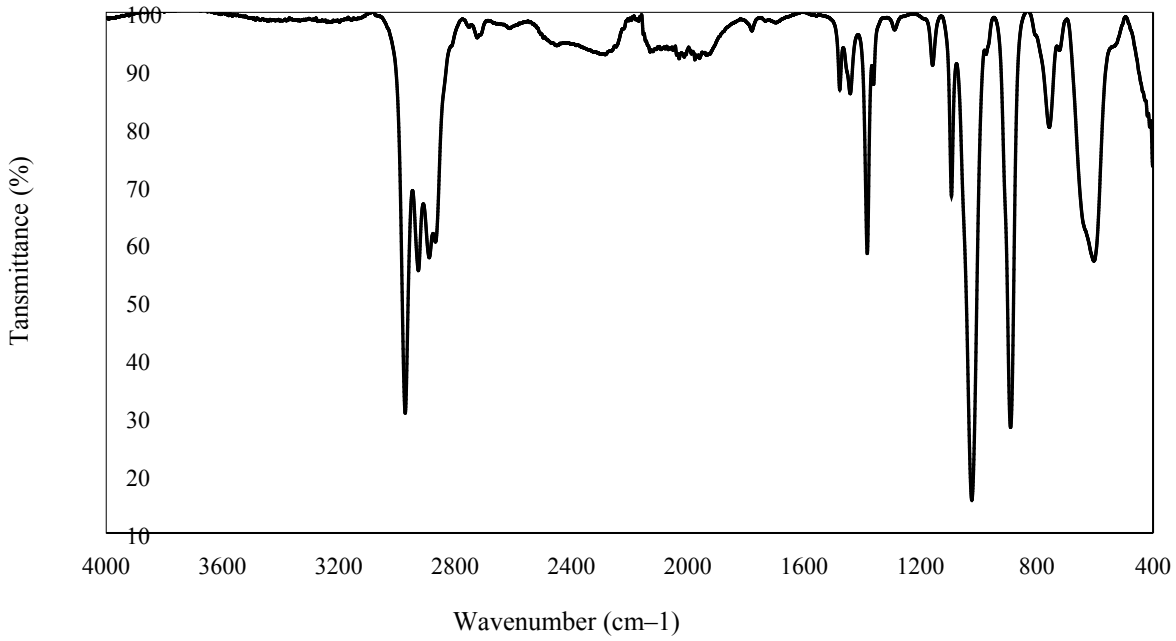

Figure S11. Di-ATR-FTIR of arsenic triethoxide.

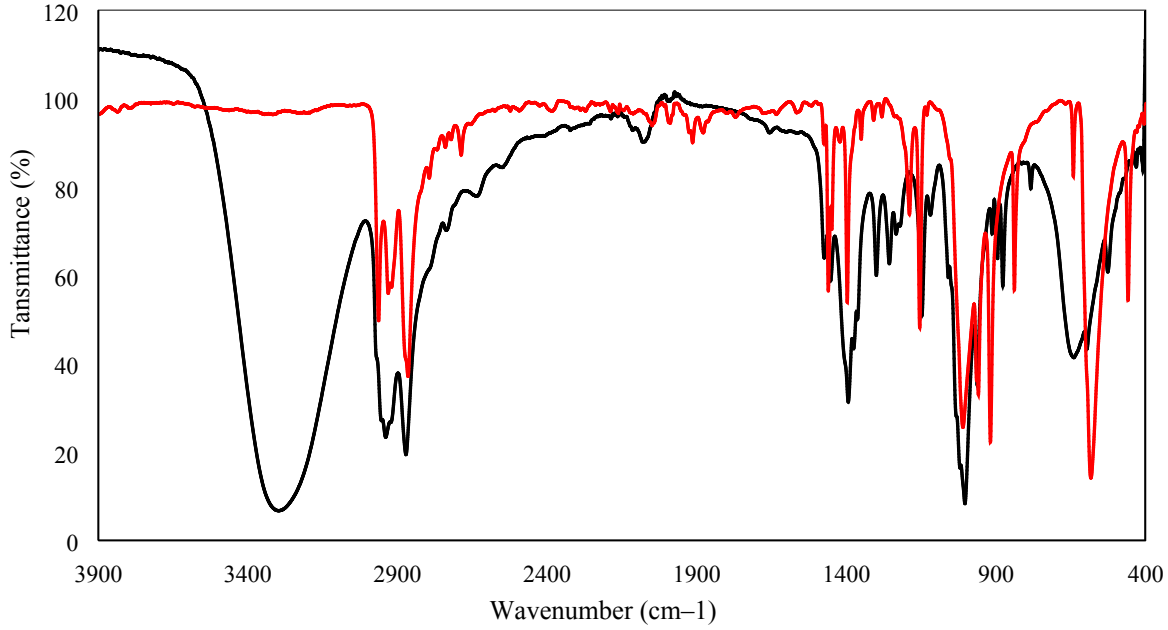

Figure S12. Di-ATR-FTIR of **4** (black) and **2**-As (red).

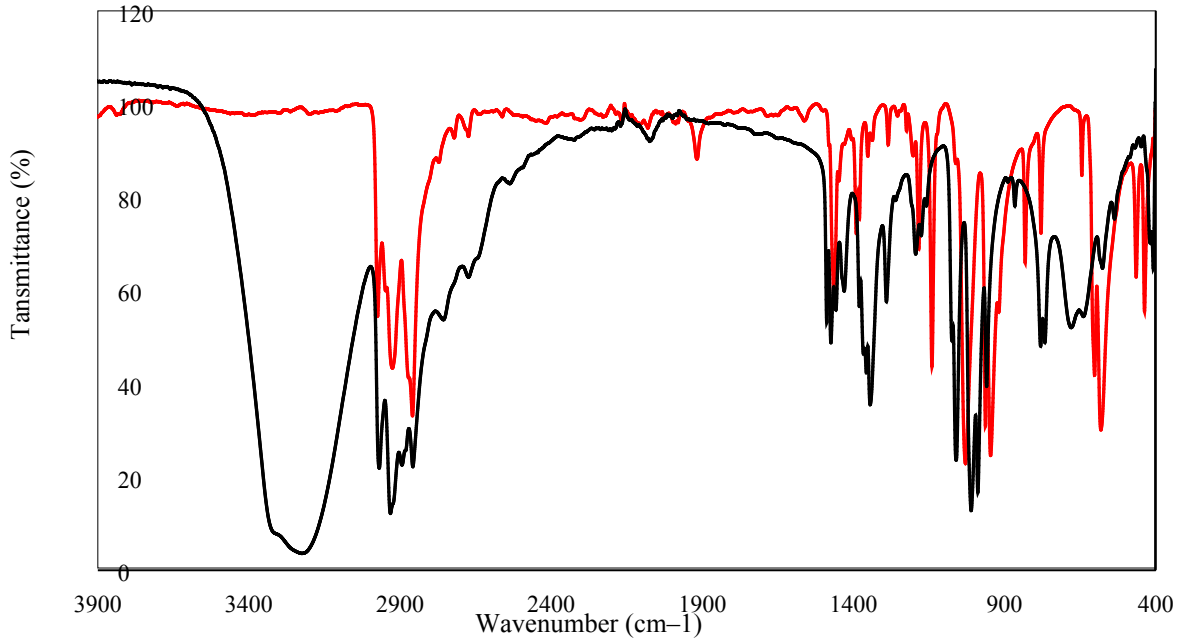

Figure S13. Di-ATR-FTIR of **5** (black) and **3**-As (red).

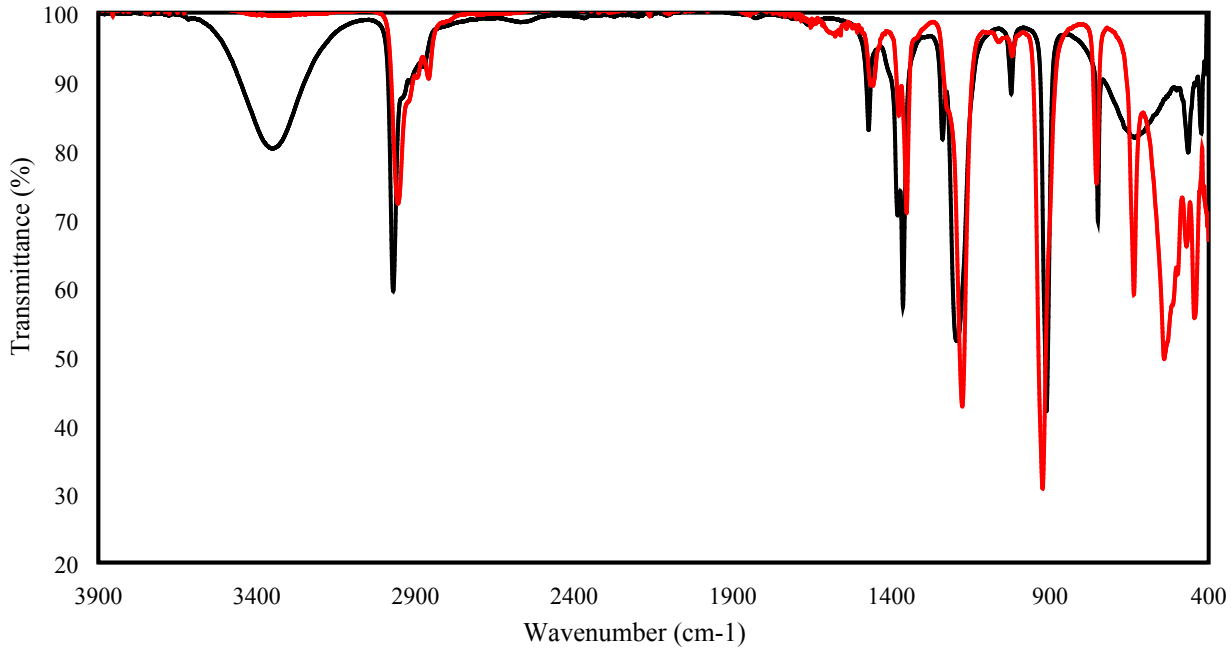

Figure S14. Di-ATR-FTIR of *tert*-butyl alcohol(black) and bismuth(III) *tert*-butoxide (red).

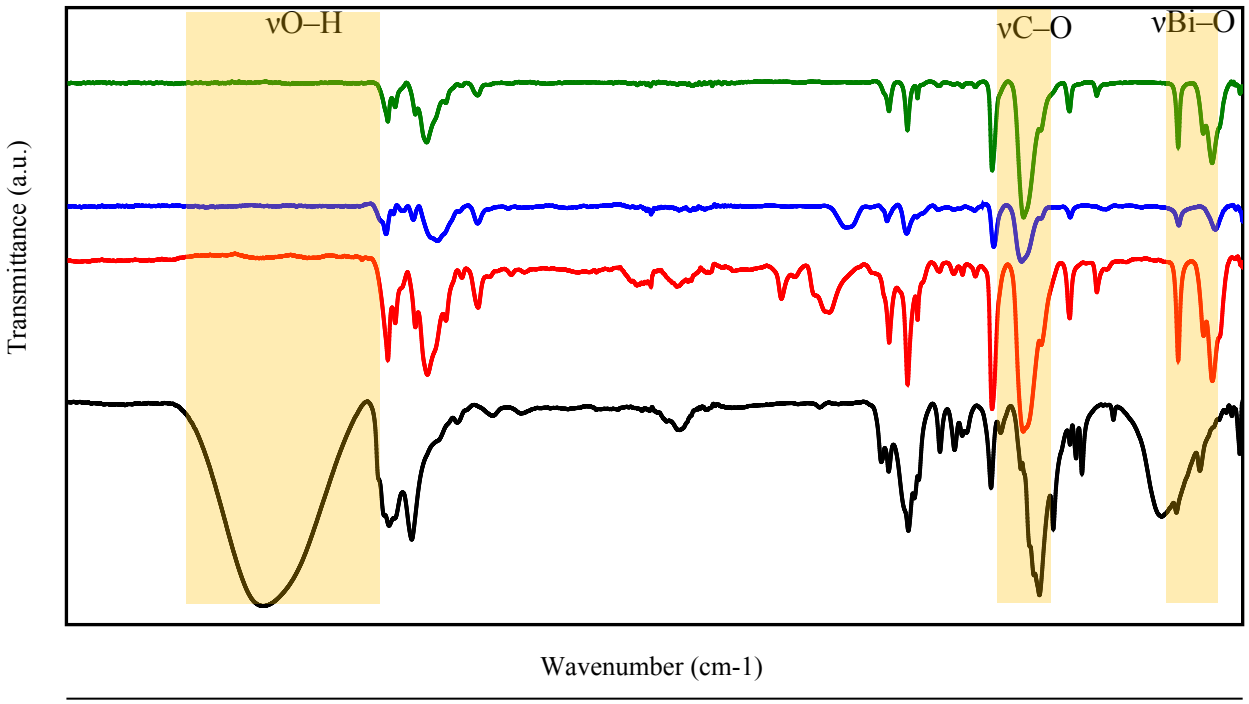

Figure S15. Di-ATR-FTIR of **4** (black) and **2**-Bi from Method A (red), Method B (blue), and Method C (green).

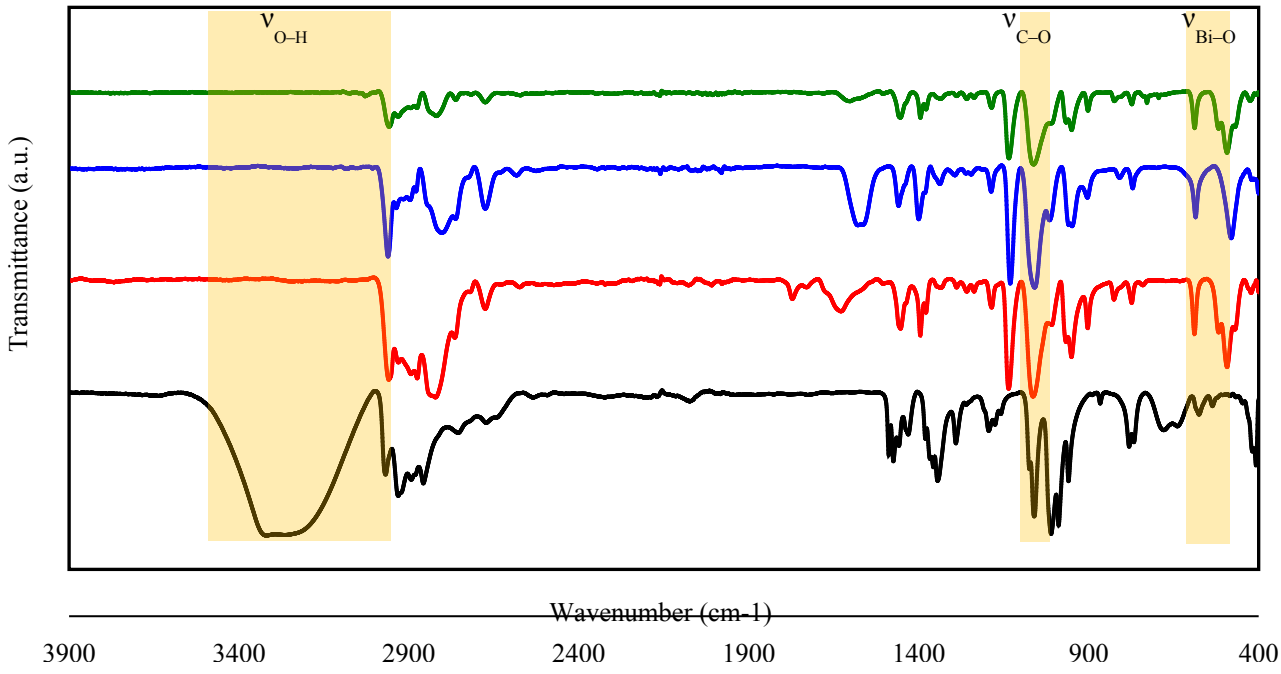

Figure S16. Di-ATR-FTIR of **5** (black) and **3**-Bi from Method A (red), Method B (blue), and Method C (green).

S2.4 Powder X-ray Diffraction

The diffraction patterns for (**2**-As and **3**-As) were collected on a Rigaku Ultima III powder diffractometer. X-ray diffraction patterns were obtained by using a 2θ scan with the source fixed at 0° and the detector scanning a θ range of 5-60°, step size = 0.02°, and scan time of 10 min/degree. The X-ray source was Cu Kα radiation (λ =1.5418 Å) with an anode voltage of 40 kV and a current of 44 mA. The beam was then discriminated by Rigaku's Cross Beam parallel beam optics to create a monochromatic parallel beam. Diffraction intensities were recorded on a scintillation detector after being filtered through a Ge monochromator.

Samples of **2**-As and **3**-As were packed inside borosilicate capillaries with inner diameter of 0.3 mm and wall thickness of 0.01 mm purchased from Charles Supper Company. Samples were prepared under inert atmosphere and the tubes were sealed with grease. After sealing they were mounted on capillary holder and data was collected. The resulting diffractograms were processed with the software JADE v9.1. Simulated patterns were obtained from single crystal data of each sample via Mercury 3.8 software. Due to the temperature difference between data acquired from the single crystals (100 K) and the PXRD samples, a slight difference between unit cells is observed.

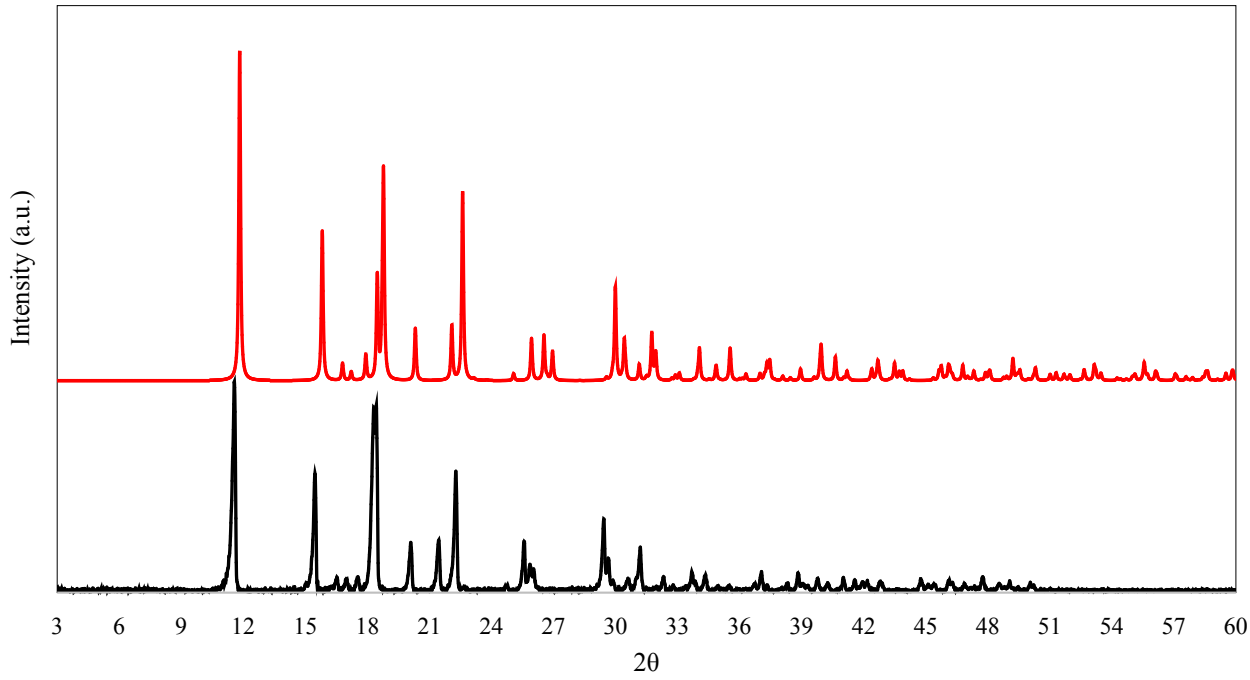

Figure S17. PXRD of **2**-As (black) and predicted pattern (red).

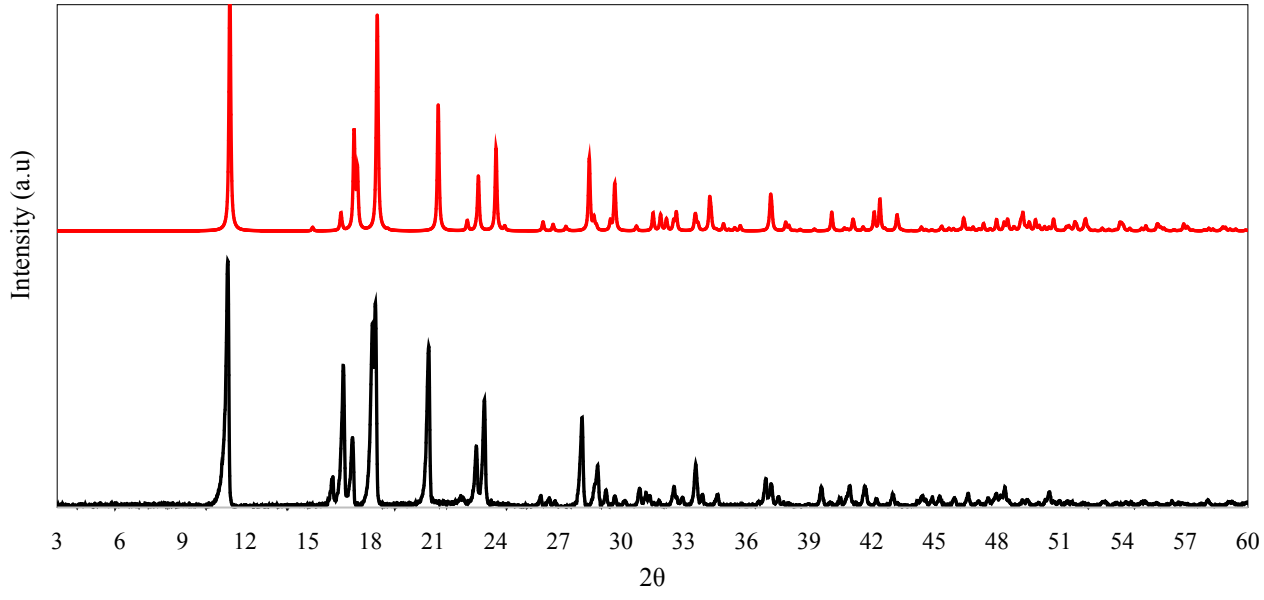

Figure S18. PXRD of **3**-As (black) and predicted pattern (red)

S3 DFT Optimized Cartesian Coordinates

See associated .zip file for all .xyz files of all optimized structures.

S4 References

(1) Clegg, William.; Compton, N. A.; Errington, R. John.; Fisher, G. A.; Green, M. E.; Hockless, D. C. R.; Norman, N. C. X-Ray Crystal Structure of Bismuth Dimethylamide. *Inorg. Chem.* **1991**, *30* (24), 4680–4682. https://doi.org/10.1021/ic00024a046.

(2) Evans, W. J.; Hain, J. H.; Ziller, J. W. Synthesis and First X-Ray Crystal Structure of a Bi(OR)3 Complex: Tris(2,6-Dimethylphenoxo)Bismuth. *J. Chem. Soc. Chem. Commun.* **1989**, No. 21, 1628–1629. https://doi.org/10.1039/C39890001628.

(3) Neese, F. Software Update: The ORCA Program System, Version 4.0. *Wiley Interdiscip. Rev. Comput. Mol. Sci.* **2018**, *8* (1), e1327. https://doi.org/10.1002/wcms.1327.

(4) Lenthe, E. van; Baerends, E. J.; Snijders, J. G. Relativistic Regular Two-component Hamiltonians. *J. Chem. Phys.* **1993**, *99* (6), 4597–4610. https://doi.org/10.1063/1.466059.

(5) Heully, J.-L.; Lindgren, I.; Lindroth, E.; Lundqvist, S.; Martensson-Pendrill, A.-M. Diagonalisation of the Dirac Hamiltonian as a Basis for a Relativistic Many-Body Procedure. *J. Phys. B At. Mol. Phys.* **1986**, *19* (18), 2799. https://doi.org/10.1088/0022-3700/19/18/011.

(6) Grimme, S.; Ehrlich, S.; Goerigk, L. Effect of the Damping Function in Dispersion Corrected Density Functional Theory. *J. Comput. Chem.* **2011**, *32* (7), 1456–1465. https://doi.org/10.1002/jcc.21759.

(7) Weigend, F.; Ahlrichs, R. Balanced Basis Sets of Split Valence, Triple Zeta Valence and Quadruple Zeta Valence Quality for H to Rn: Design and Assessment of Accuracy. *Phys. Chem. Chem. Phys.* **2005**, *7* (18), 3297–3305. https://doi.org/10.1039/B508541A.

(8) Schafer, A.; Horn, H.; Ahlrichs, R. Fully Optimized Contracted Gaussian Basis Sets for Atoms Li to Kr. *J. Chem. Phys.* **1992**, *97* (4), 2571–2577. https://doi.org/10.1063/1.463096.

(9) Weigend, F. Accurate Coulomb-Fitting Basis Sets for H to Rn. *Phys. Chem. Chem. Phys.* **2006**, *8* (9), 1057–1065. https://doi.org/10.1039/B515623H.

(10) Kohn, W.; Sham, L. J. Self-Consistent Equations Including Exchange and Correlation Effects. *Phys. Rev.* **1965**, *140* (4A), A1133–A1138. https://doi.org/10.1103/PhysRev.140.A1133.

(11) Kendall, R. A.; Früchtl, H. A. The Impact of the Resolution of the Identity Approximate Integral Method on Modern Ab Initio Algorithm Development. *Theor. Chem. Acc.* **1997**, *97* (1), 158–163. https://doi.org/10.1007/s002140050249.

(12) Boys, S. F.; Bernardi, F. The Calculation of Small Molecular Interactions by the Differences of Separate Total Energies. Some Procedures with Reduced Errors. *Mol. Phys.* **1970**, *19* (4), 553–566. https://doi.org/10.1080/00268977000101561.

(13) Lu, T.; Chen, F. Quantitative Analysis of Molecular Surface Based on Improved Marching Tetrahedra Algorithm. *J. Mol. Graph. Model.* **2012**, *38*, 314–323. https://doi.org/10.1016/j.jmgm.2012.07.004.

(14) Lu, T.; Chen, F. Multiwfn: A Multifunctional Wavefunction Analyzer. *J. Comput. Chem.* **2012**, *33* (5), 580–592. https://doi.org/10.1002/jcc.22885.

(15) Allouche, A.-R. Gabedit—A Graphical User Interface for Computational Chemistry Softwares. *J. Comput. Chem.* **2011**, *32* (1), 174–182. https://doi.org/10.1002/jcc.21600.